Supporting Information

containing 14 pages, with 4 figures

to accompany the manuscript entitled

Iron Redox Transformations in Continuously Photolyzed Acidic Solutions Containing Natural Organic Matter: Kinetic and Mechanistic Insights

Shikha Garg[1], Chao Jiang[1], Christopher J. Miller[1], Andrew L. Rose[2]

and T. David Waite[1]*

[1]*School of Civil and Environmental Engineering, The University of New South Wales, Sydney, NSW 2052, Australia*

[2]*Southern Cross GeoScience, Southern Cross University, Lismore NSW 2480, Australia*

Resubmitted

Environmental Science and Technology

July 2013

*Corresponding author: Phone +61-2-9385 5059, FAX +61-2-9385 6139, Email d.waite@unsw.edu.au

SI-1: Experimental method details

SI-1.1: Stability of SRFA solution

The stability of pH 4 SRFA solutions of different concentrations (2.5-10 mg.L^{-1}) was examined and properties found to be stable over timescales typical of the experiments undertaken here (10 min – 24 h). Specifically, the SRFA absorbance did not change over time periods of up to 24 h and the rate of H_2O_2 production on photolysis of SRFA solutions that had been prepared 24 h earlier was identical to that of freshly prepared SRFA solutions. Furthermore, Fe(II) oxidation and Fe(III) reduction rates for SRFA solutions that had been prepared 24 h earlier were identical to those of freshly prepared SRFA solutions.

SI-1.2: Fe(II) generation kinetics from Fe(III) reduction and Fe(II) oxidation kinetics in photolyzed SRFA solution

Fe(II) generation kinetics were measured during photolysis of SRFA solutions containing Fe(III), while Fe(II) oxidation kinetics were measured during photolysis of SRFA solutions with addition of Fe(II). In all cases, 3 mL of solution containing SRFA and Fe(III) was photolyzed in a 1 cm quartz cuvette for 0.5, 1, 2, 5, or 10 min followed by addition of 60 µL FZ-DFB mix, with Fe(II) concentrations at each time point determined using the modified FZ method described in our earlier study [1]. Both types of experiment were conducted with a range of additional treatments:

1. Addition of 12.5 and 25 kU.L^{-1} SOD, with 5 or 10 mg.L^{-1} SRFA and either 100 nM total Fe(III) (for Fe(III) reduction kinetics) or 100 nM total Fe(II) (for Fe(II) oxidation kinetics). Fe(II) and Fe(III) calibrations were performed in the presence of SOD and the molar absorption coefficient obtained was the same in the presence and absence of SOD, supporting the conclusion that SOD does not react with Fe present in our experimental matrix. Furthermore, in control experiments where SOD was added to solutions containing Fe(II) or

Fe(III) in the absence of SRFA (under both non-irradiated and irradiated conditions), no change in Fe(II) or Fe(III) concentrations was observed (data not shown).

2. Substitution of D_2O for water, with 10 mg.L^{-1} SRFA and either 100 nM of Fe(III) (for Fe(III) reduction kinetics) or 100 nM total Fe(II) (for Fe(II) oxidation kinetics). Calibration was performed by standard addition of Fe(II) or Fe(III) to SRFA solution adjusted to pD 4 prepared in 99.9% D_2O and was similar to that in aqueous solution. Correction was employed for the pD-pH effect. Control experiments measuring Fe(III) reduction kinetics and Fe(II) oxidation kinetics in the dark in D_2O solution in the absence of SRFA were also performed. No change in Fe(II) concentration was observed (data not shown), confirming that no transformation of Fe(II) or Fe(III) occurred in D_2O solution in the dark and in the absence of SRFA.

3. Addition of DMSO, with 5 mg.L^{-1} SRFA and either 100 nM Fe(III) (for Fe(III) reduction kinetics) or 100 nM total Fe(II) (for Fe(II) oxidation kinetics). Both Fe(II) and Fe(III) calibrations were performed in the presence of DMSO and the molar absorption coefficient obtained was found to be identical in the presence and absence of DMSO with this result supporting the conclusion that DMSO does not react with the Fe present in our experimental matrix. Furthermore, in control experiments where DMSO was added to solutions containing Fe(II) or Fe(III) in the absence of SRFA (under both non-irradiated and irradiated conditions), no change in Fe(II) or Fe(III) concentrations was observed (data not shown).

SI-2: Additional manipulative experiments to probe the nature and mechanism of generation of Fe(II) oxidant unlikely
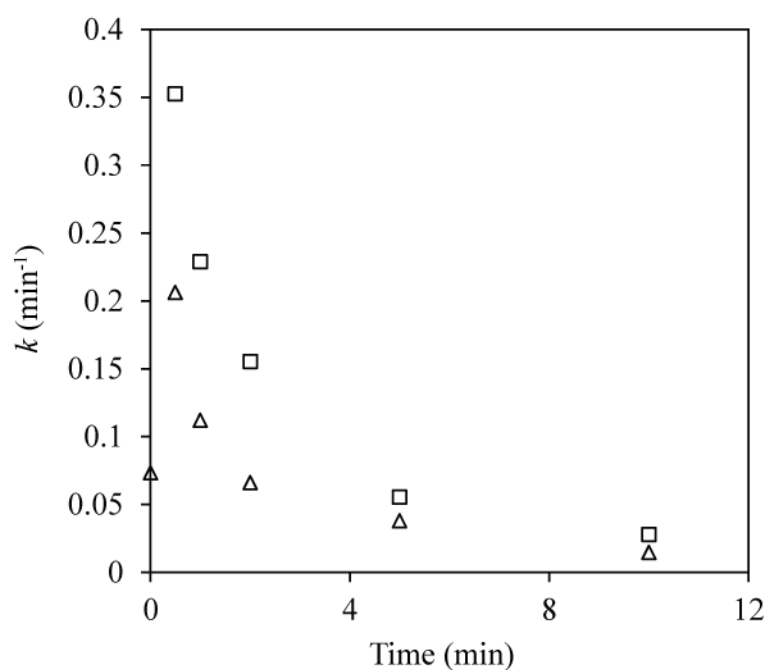

Figure SI-1: Calculated pseudo-first rate constant (k) for oxidation of 100 nM (squares) and 50 nM (triangles) in irradiated solutions containing 5 mg.L^{-1} SRFA as a function of time.
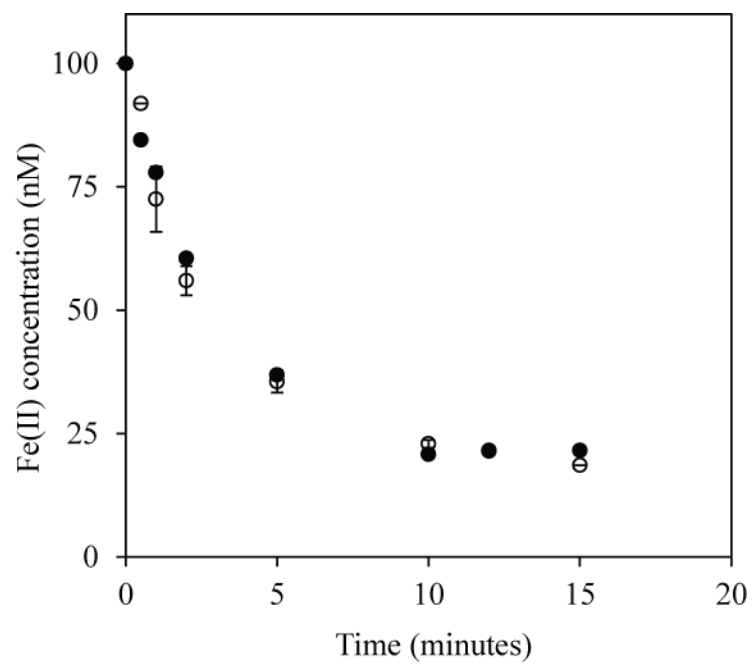
Figure SI-2: Fe(II) oxidation kinetics in irradiated 10 mg.L^{-1} SRFA solution in the absence (open circles) and presence (closed circles) of 2 µM H_2O_2
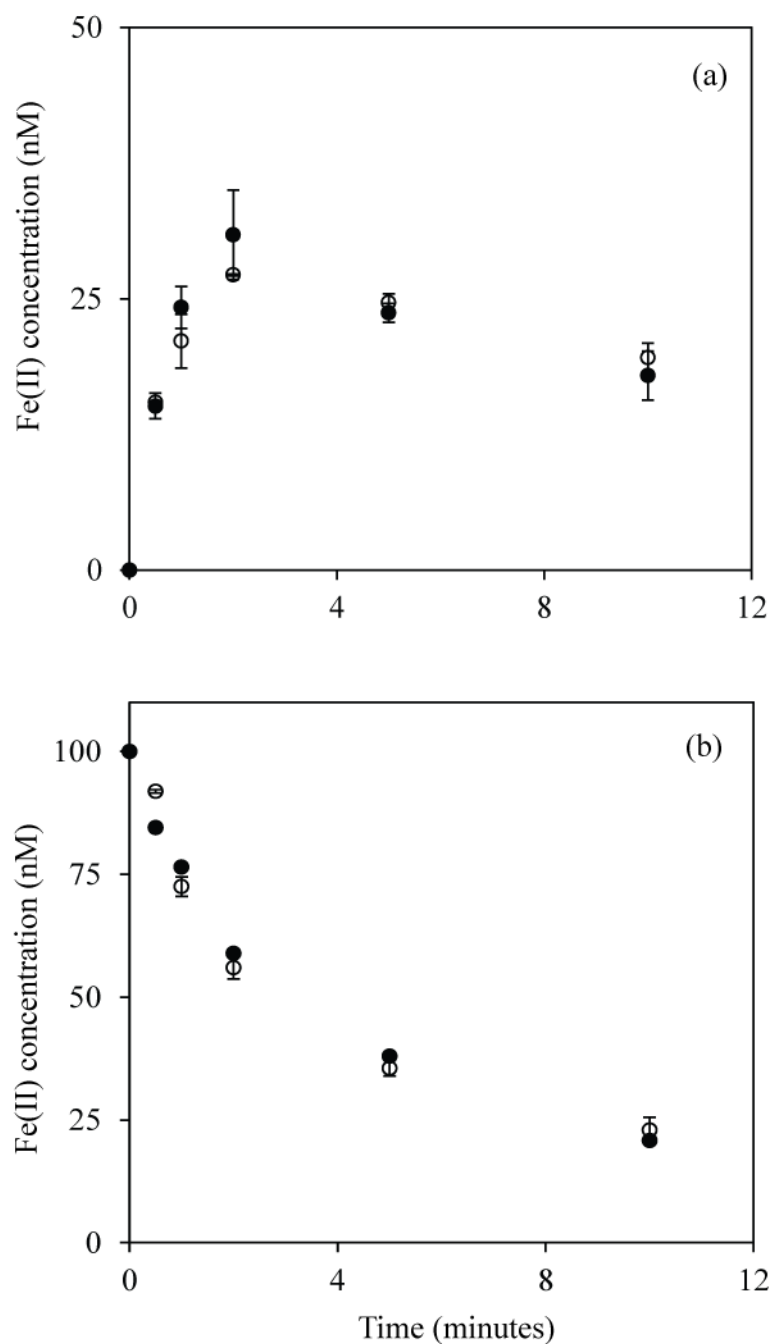
Figure SI-3 (a) Photochemical generation of Fe(II) following addition of 100 nM Fe(III) to 5 mg.L^{-1} SRFA in air saturated aqueous solution (open circles) and air saturated D$_2$O solution (closed circles); (b) Photochemical Fe(II) oxidation following addition of 100 nM Fe(II) to 5 mg.L^{-1} SRFA in air saturated aqueous solution (open circles) and air saturated D$_2$O solution (closed circles). Symbols represent experimental data (average of duplicate measurements).
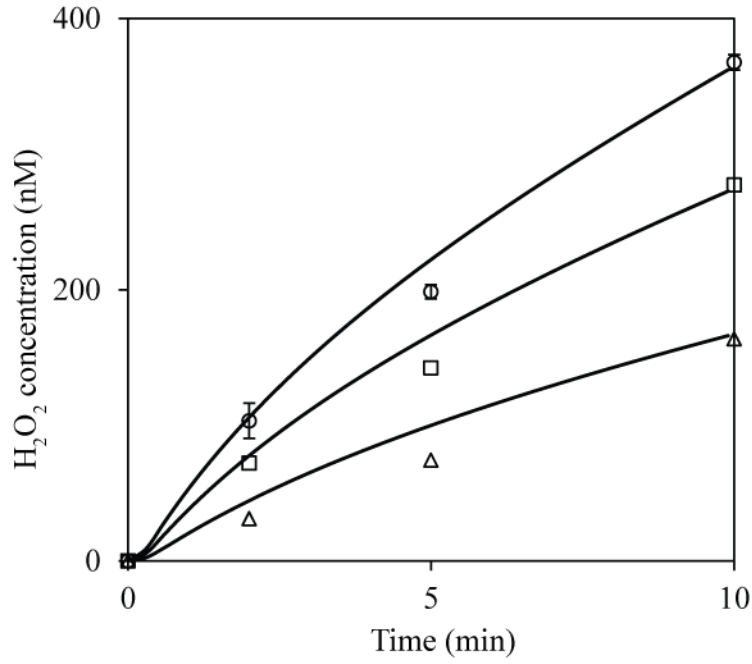
Figure SI-4: H_2O_2 concentration generated from photolysis of 2.5 mg.L^{-1} (triangles), 5 mg.L^{-1} (squares) and 10 mg.L^{-1} (circles) SRFA for 10 min. Symbols represent the average of duplicate measurements; lines represent model values.

SI-3: Details of the kinetic model

Based on the analysis presented in the manuscript and our earlier work on Fe redox transformations in previously photolysed SRFA solution [1] and photochemical generation of ROS on SRFA photolysis [2], a kinetic model was developed to describe Fe redox transformation in continuously irradiated SRFA solutions. The main features of the kinetic model (see Table 1 in the main text) are discussed in detail below.

SI-3.1   Instantaneous establishment of steady-state singlet oxygen concentration

$^1O_2$ reaches a steady-state concentration almost instantaneously due to its rapid formation via reaction of $^3O_2$ with photoexcited SRFA (eq. 1) and relaxation of the excited singlet state in solution (eq. 2):

$$SRFA + h\nu \longrightarrow SRFA^* \xrightarrow{^3O_2} {}^1O_2 + SRFA$$

(1)

$$^1O_2 \xrightarrow{\;H_2O\;} {}^3O_2 \tag{2}$$

The rate constant for the reaction shown in eq. 1 was calculated based on the photon absorption rate by SRFA as described in our earlier work. The rate constant for the relaxation reaction (eq. 2) was determined assuming that relaxation of $^1O_2$ mainly occurs via its interaction with the solvent, with a rate constant of 2.4×10^5 s^{-1} in aqueous solution and 1.5×10^4 s^{-1} in D$_2$O solution (since the lifetime of $^1O_2$ is 16-fold higher in D$_2$O solution compared to aqueous solution) [3]. Rate constants for both these reactions were fixed during modeling.

SI-3.2   Superoxide formation during irradiation

Superoxide formation during irradiation was modelled using the reactions:

$$Q + h\nu \xrightarrow{\;e^-\;} Q^- \tag{3}$$

$$Q^- + {}^3O_2 \longrightarrow Q + HO_2^{\bullet} \tag{4}$$

$$Q^- \longrightarrow NRP \tag{5}$$

where NRP represents a non-reactive product.

Photoexcitation of Q followed by electron transfer or H abstraction results in formation of the O_2-reducing radical Q^-. The reaction shown in eq. 5 is an apparent reaction incorporating excitation of Q, relaxation to ground state and reduction of the excited state by an electron donor. The apparent rate constant for reduction of Q to Q^- was determined based on best-fit to the H$_2$O$_2$ generation data shown in Fig. SI-4 assuming that the initial concentration of Q was proportional to the SRFA concentration. A total concentration of 1.7 mmol.g^{-1} SRFA was used for modelling based on the reported electron accepting capacity of quinone moieties in humic and fulvic acids [4]. However, the initial concentration of Q is not well constrained

by our experimental data, with a similar fit able to be obtained for varying concentrations with suitable adjustment of the rate constant for the reaction in eq. 3. The same rate constant for the reaction shown in eq. 4 as used by Zhang et al. [5] for reaction of O_2 with either an excited triplet state or a reducing radical intermediate based on results of earlier investigators was used here. The reaction shown in eq. 5 represents relaxation of Q^- to form a non-reactive product (NRP) with the rate constant for this reaction determined using the measured effect of dioxygen removal on H_2O_2 formation rate (see [1]) as described by Zhang and co-workers [5]. The H_2O_2 formation rate decreased by ~30% after 95% removal of dioxygen, which yields a ratio of 1.7×10^5 M for the rate constants for the reactions shown in eqs 4 and 5. Using the value of 1×10^9 $M^{-1}.s^{-1}$ assumed by Zhang and co-workers [5] for the rate constant for reaction 4, we obtain a value of 5.8×10^3 s^{-1} for the rate constant for reaction 5. This implies that the lifetime of Q^- is ~173 μs which is consistent with the finding that the reactive intermediate responsible for H_2O_2 production is relatively stable in the absence of dioxygen [5]. The lifetime of Q^- determined here is about 6-times higher than the value reported by Zhang and co-workers [5], which may be due to differences in pH, experimental matrix and light intensity used in the two studies. It is to be noted however that the lifetime of Q^- (which controls superoxide generation rate) has minimal effect on the modelled Fe redox transformations in this study since the major pathways for both Fe(III) reduction and Fe(II) oxidation are superoxide-independent.

A constant $HO_2^\bullet$ generation rate is most consistent with experimental data in this and earlier work [2] in which $HO_2^\bullet$ concentrations reached steady-state after 10–20 min. If the $HO_2^\bullet$ generation rate was to decrease over time due to consumption of Q, a steady-state $HO_2^\bullet$ concentration would not be observed. Thus, in order to maintain a constant $HO_2^\bullet$ generation rate, we have assumed that Q is regenerated when Q^- reacts with dioxygen, which is

consistent with Q^- being similar to semiquinone-like radicals. This is also consistent with recent studies showing that, once reduced, electron accepting quinone moieties in humic and fulvic substances can be reoxidized by dioxygen [4, 6]. Furthermore, in order to maintain a constant $HO_2^{\bullet}$ generation rate, a continuous source of electrons is required for reduction of Q. Based on the kinetic model, we require an electron donor concentration of at least 1 mmol.g^{-1} SRFA if this donor is irreversibly consumed. This value is consistent with the recently reported electron donating capacity of humic and fulvic acids [7].

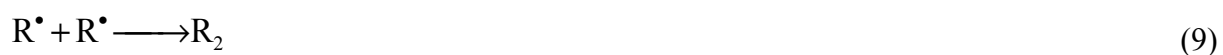*SI-3.3   Uncatalyzed disproportionation of superoxide*

Superoxide (or, rather, at pH 4, the hydroperoxy radical) undergoes uncatalyzed disproportionation in the dark to form H_2O_2. The rate constant for this reaction was used as reported earlier at pH 4 [8].

$$HO_2^{\bullet} + HO_2^{\bullet} \longrightarrow O_2 + H_2O_2 \tag{6}$$

This uncatalyzed process will be unimportant in the light since, under these conditions, the disproportionation of the hydroperoxy radical will be catalyzed by the presence of iron.

SI-3.4   Oxidative superoxide sink

During irradiation, a substantial amount of $HO_2^{\bullet}$ decays via an oxidative pathway, as demonstrated by the increase in H_2O_2 production rates on addition of SOD (see [1]). The following reactions were included in the model to account for this oxidative sink of $HO_2^{\bullet}$:

$$R + h\nu \longrightarrow R^{\bullet} \tag{7}$$

$$R^{\bullet} + HO_2^{\bullet} \longrightarrow R^- + O_2 \tag{8}$$

$$R^{\bullet} + R^{\bullet} \longrightarrow R_2 \tag{9}$$

The rate constants for the reactions shown in eqs. 8 and 9 were used as determined in our earlier work [2] based on best fit to the $HO_2^{\bullet}$ concentration profile during irradiation and after the lamp was extinguished while the rate constant for reaction 7 was determined based on best-fit to our experimental data.

SI-3.5 A^- generation

As discussed in our earlier work [1], $HO_2^{\bullet}$ oxidizes the reduced organic group (A^{2-}) to form A^-, which can further undergo reaction with $HO_2^{\bullet}$ to catalyse its disproportionation in the dark or can also be oxidized by $^1O_2$ under irradiated conditions according to the following reactions:

$$A^{2-} + HO_2^{\bullet} \longrightarrow A^- + H_2O_2 \tag{10}$$

$$A^- + HO_2^{\bullet} \longrightarrow A^{2-} + O_2 \tag{11}$$

$$A^- + {}^1O_2 \longrightarrow A + HO_2^{\bullet} \tag{12}$$

The rate constant for the reaction shown in eq. 10 was determined based on the values reported in the literature [9] as well as in our earlier work [2]. The rate constants for the reactions shown in eq. 11 and 12 were determined based on best-fit to experimental data for Fe(II) oxidant generation in previously photolyzed SRFA solution from earlier work [1]. The total initial concentration of A^{2-} was used as calculated (i.e. 35.4 $\mu mol.g^{-1}$ SRFA) based on the measured steady-state concentration of Fe(II) generated on Fe(III) reduction in SRFA solution in the dark [1].

 SI-3.6   Peroxyl radical generation

As shown in eq. 13, hydroxyl radicals or hydroxylating intermediates formed on photolysis of SRFA react with bulk organic matter resulting in the formation of carbon-centered radicals which further react with O_2 irreversibly, forming corresponding peroxyl radicals [10]. Peroxyl radicals so formed can undergo bimolecular or unimolecular decay [10]:

$$R + h\nu \xrightarrow{\quad O_2, OH^\bullet \quad} RO_2^\bullet \tag{13}$$

$$RO_2^\bullet + RO_2^\bullet \longrightarrow RO_4R \tag{14}$$

$$RO_2^\bullet \longrightarrow R^{\bullet+} + HO_2^\bullet \tag{15}$$

The rate constants for the reactions shown in eqs. 13 and 15 were determined based on best-fit to experimental data for Fe redox transformation in continuously irradiated SRFA solution while the rate constant for the reaction shown in eq. 14 was used as reported earlier [11].

SI-3.7 Fe redox transformations by reaction with A^- and A^{2-} in continuously irradiated SRFA solution

Reactions shown in eq. 16 and 17 show Fe(II) oxidation by A^- and Fe(III) reduction by A^{2-}. The rate constants for these reactions determined in our earlier work [1] were used here.

$$Fe(II) + A^- \longrightarrow Fe(III) + A^{2-} \tag{16}$$

$$Fe(III) + A^{2-} \longrightarrow Fe(II) + A^- \tag{17}$$

SI-3.8 Fe(II) oxidation by peroxyl radicals in continuously irradiated SRFA solution

The reaction shown in eq. 18 represents oxidation of Fe(II) by peroxyl radicals. The rate constant for this reaction was determined based on best-fit to experimental data and is within the range of previously published values [12].

$$\text{Fe(II)} + \text{RO}_2^\bullet \longrightarrow \text{Fe(III)} + \text{RO}_2\text{H} \tag{18}$$

SI: 3.9 Fe(III) reduction by LMCT in continuously irradiated SRFA solution

The reaction in eq. 19 shows reduction of Fe(III) by LMCT with the rate constant determined by best-fit to experimental data.

$$\text{Fe(III)} \xrightarrow{\text{hv,L}} \text{Fe(II)} + \text{L}_{ox} \tag{19}$$

SI: 3.10 Fe redox transformations by reaction with superoxide in continuously irradiated SRFA solution

The reactions shown in eqs. 20 and 21 represent superoxide-mediated Fe(III) reduction and Fe(II) oxidation respectively. The rate constant for SMIR was used as reported earlier for Fe(III)SRFA at pH 8 [13]. The rate constant for superoxide-mediated Fe(II) oxidation was used as reported for inorganic Fe(II) at pH 4 [14].

$$\text{Fe(III)} + \text{HO}_2^\bullet \longrightarrow \text{Fe(II)} + \text{O}_2 \tag{20}$$

$$\text{Fe(II)} + \text{HO}_2^\bullet \longrightarrow \text{Fe(III)} + \text{H}_2\text{O}_2 \tag{21}$$

SI-4: Relative contributions of Fe(III) reduction by LMCT, SMIR and A^{2-}

The relative contributions of these processes to overall Fe(III) reduction are given by:

$$\text{Relative contribution of LMCT to Fe(III) reduction} = \frac{k_{psuedo}^{LMCT}}{k_{psuedo}^{LMCT} + k_{psuedo}^{SMIR} + k_{psuedo}^{A^{2-}}} \tag{22}$$

$$\text{Relative contribution of SMIR to Fe(III) reduction} = \frac{k_{\text{psuedo}}^{\text{SMIR}}}{k_{\text{psuedo}}^{\text{LMCT}} + k_{\text{psuedo}}^{\text{SMIR}} + k_{\text{psuedo}}^{\text{A}^{2-}}} \tag{23}$$

$$\text{Relative contribution of A}^{2\text{-}} \text{ to Fe(III) reduction} = \frac{k_{\text{psuedo}}^{\text{A}^{2-}}}{k_{\text{psuedo}}^{\text{LMCT}} + k_{\text{psuedo}}^{\text{SMIR}} + k_{\text{psuedo}}^{\text{A}^{2-}}} \tag{24}$$

where $k_{\text{psuedo}}^{\text{LMCT}}$, $k_{\text{psuedo}}^{\text{SMIR}}$, and $k_{\text{psuedo}}^{\text{A}^{2-}}$ are the pseudo-first order rate constants for Fe(III) reduction by LMCT, SMIR and A^{2-} respectively. $k_{\text{psuedo}}^{\text{LMCT}} = 7.5 \times 10^{-3}$ s^{-1} for all SRFA concentrations, while the values for $k_{\text{psuedo}}^{\text{SMIR}}$ and $k_{\text{psuedo}}^{\text{A}^{2-}}$ were calculated using the modeled rate constants for Fe(III) reduction by superoxide and A^{2-} and the model predicted average concentrations of superoxide and $A^{2-,-}$ respectively.

References

1.   Garg, S.; Ito, H.; Rose, A. L.; Waite, T. D., Mechanism and kinetics of dark iron redox transformations in previously photolyzed acidic natural organic matter solutions. *Environ. Sci. Technol* **2013**, *47*, 1861−1869.

2.   Garg, S.; Rose, A. L.; Waite, T. D., Photochemical production of superoxide and hydrogen peroxide from natural organic matter. *Geochim Cosmochim Acta* **2011,** *74*, 4310-4320.

3.   Wilkinson, F.; Helman, W. P.; Ross, A. B., Rate constants for the decay and reactions of the lowest electronically excited singlet state of molecular oxygen in solution. An expanded and revised compilation. *J Phys Chem Ref Data* **1995,** *24*, 663.

4.   Aeschbacher, M.; Vergari, D.; Schwarzenbach, R. P.; Sander, M., Electrochemical analysis of proton and electron transfer equilibria of the reducible moieties in humic acids. *Environ. Sci. Technol* **2011,** *45*, 8385-8394.

5.   Zhang, Y.; Vecchio, R. D.; Blough, N. V., Investigating the mechanism of hydrogen peroxide photoproduction by humic substances. *Environ. Sci. Technol* **2012,** *46*, 11836-11843.

6.   Aguirre, J.; Rios-Momberg, M.; Hewitt, D.; Hansberg, W., Reactive oxygen species and development in microbial eukaryotes. *Trends in Microbiology* **2005,** *13*, 111-118.

7.   Aeschbacher, M.; Graf, C.; Schwarzenbach, R. P.; Sander, M., Antioxidant properties of humic substances. *Environ. Sci. Technol* **2012,** *46*, 4916-4925.

8.   Bielski, B. H. J.; Cabelli, D. E.; Arudi, R. L.; Ross, A. B., Reactivity of HO_2/O_2^- radicals in aqueous solution. *J Phys Chem Ref Data* **1985,** *14*, 1041-1100.

9.   Roginsky, V.; Barsukova, T., Kinetics of oxidation of hydroquinones by molecular oxygen. Effect of superoxide dismutase *Journal of Chemical Society - Perkin Transaction II* **2000,** *2000*, 1575-1582.

10.   von Sonntag, C.; Dowideit, P.; Fang, X.; Mertens, R.; Pan, X.; Schuchmann, M. N.; Schuchmann, H.-P., The fate of peroxyl radicals in aqueous solution. *Water Science and Technology* **1997,** *35*, 9-15.

11.   Neta, P.; Huie, R. E.; Ross, A. B., Rate constants for reactions of peroxyl radicals in fluid solutions. *J Phys Chem Ref Data* **1990,** *19*, 413.

12.   Khaiken, G. I.; Alfassi, Z. B.; Huie, R. E.; Neta, P., Oxidation of ferrous and ferrocyanide ions by peroxyl radicals. *J Phys Chem* **1996,** *100*, 7072-7077.

13.   Garg, S.; Rose, A. L.; Waite, T. D., Superoxide mediated reduction of organically complexed iron(III): Comparison of non-dissociative and dissociative reduction pathways. *Environ. Sci. Technol.* **2007,** *41*, 3205-3212.

14.   Rush, J. D.; Bielski, B. H. J., Pulse radiolytic studies of the reactions of HO_2/O_2^- with Fe(II)/Fe(III) ions. The reactivity of HO_2/O_2^- with ferric ions and its implication on the occurrence of the Haber-Weiss reaction. *J Phys Chem* **1985,** *89*, 5062-5066.